J|A|C|S
ARTICLES
Published on Web 01/18/2003

Trends in Metal−Biradical Exchange Interaction for First-Row M^{II}(Nitronyl Nitroxide-Semiquinone) Complexes

David A. Shultz,*,† Kira E. Vostrikova,† Scot H. Bodnar,† Hyun-Joo Koo,† Myung-Hwan Whangbo,*,† Martin L. Kirk,*,‡ Ezra C. Depperman,‡ and Jeff W. Kampf§

Contribution from the Department of Chemistry, North Carolina State University, Raleigh, North Carolina 27695-8204, Department of Chemistry, University of New Mexico, Albuquerque, New Mexico 87131, and Department of Chemistry, University of Michigan, Ann Arbor, Michigan 48109-1055

Received May 21, 2002; Revised Manuscript Received November 1, 2002; E-mail: david_shultz@ncsu.edu; mike_whangbo@ncsu.edu; mkirk@unm.edu

Abstract: We report molecular structures and temperature-dependent magnetic susceptibility data for several new metal complexes of heterospin triplet ground-state biradical ligands. The ligands are comprised of both nitronyl-nitroxide (NN) and semiquinone (SQ) spin carriers. Five compounds are five-coordinate M^{II} complexes (M = Mn, Co, Ni, Cu, and Zn), and one is a six-coordinate Ni^{II} complex. Five compounds were structurally characterized. During copper complex formation a reaction with methanol occurs to form a unique methoxy-substituted SQ ring. Variable-temperature magnetic susceptibility studies are consistent with strong intraligand (NN-SQ and NN-PhSQ) ferromagnetic exchange coupling. For the five-coordinate Mn, Co, and Ni complexes, the $S = 1$ ligand is antiferromagnetically coupled to the metal. For both the five-coordinate Cu complex and the six-coordinate Ni complex, the ligand is ferromagnetically coupled to the metal spins in accordance with orbital symmetry arguments. Despite the low molecular symmetries, the predicted trend in metal−ligand exchange interactions is supported by spin dimer analysis based on extended Hückel calculations. For **(NN-SQ)NiTp^{Cum,Me}** (**Tp^{Cum,Me}** = hydro-tris(3-cumenyl-5-methylpyrazolyl)-borate), an antisymmetric exchange term was required for the best fit of the magnetic susceptibility data. Antisymmetric exchange was less important for the other complexes due to inherently smaller Δg. Finally, it is shown that intraligand exchange coupling is of paramount importance in stabilizing high-spin states of mixed metal−biradical complexes.

Introduction

Recent efforts in molecular magnetism have produced a plethora of fascinating molecule-based materials.[1] One of the most productive research areas in modern magnetochemistry has been preparation and study of Prussian blue analogues. This class of coordination polymers derives interesting and novel properties from superexchange interactions mediated by bridging cyanide. Interesting properties such as high-temperature magnetic ordering ($T \geq 300$ K),[2] photomagnetism,[3] and electromagnetism[4] have been discovered and studied.

However, coordination polymers comprised of diamagnetic ligands only slightly larger than cyanide (e.g., oxalate and azide[5]) do not magnetically order at temperatures above ca. 40 K.[6,7] This is due to the far weaker superexchange interactions that are attenuated by larger diamagnetic ligands[8] and due to low lattice dimensionality.

Weaker superexchange via large diamagnetic ligands can be circumvented by using paramagnetic ligands. In this way the inherently weaker superexchange interactions are dominated by direct exchange between the metal and the paramagnetic ligand. The most common paramagnetic ligands include TCNE radical anion,[9] nitroxide-type radicals,[10,11] semiquinones,[12] and several interesting new verdazyl-type molecules.[13] Application of the

* To whom correspondence should be addressed. Telephone: (919) 515-6972 (D.A.S.); (919) 515-3464 (M.-H.W.); (505) 277-5992 (M.L.K.). Fax: (919) 515−8920 (D.A.S.); (505) 277-2609 (M.L.K.). Web: http://www.ncsu.edu/chemistry/das.html (D.A.S.); http://www.ncsu.edu/chemistry/mhw.html (M.-H.W.); http://www.unm.edu/~graduate/research/kirk.html (M.L.K.).
† North Carolina State University.
‡ University of New Mexico.
§ University of Michigan.

(1) Miller, J. S.; Drillon, M. *Magnetism: Molecules to Materials II: Molecule-Based Materials*; Wiley-VCH: New York, 2001; p 489.
(2) Ferlay, S.; Mallah, T.; Ouahes, R.; Veillet, P.; Verdaguer, M. *Nature* **1995**, *378*, 701.
(3) Sato, O.; Iyoda, T.; Fujishima, A.; Hashimoto, K. *Science* **1996**, *272*, 704.
(4) Sato, O.; Iyoda, T.; Fujishima, A.; Hashimoto, K. *Science* **1996**, *271*, 49.
(5) Ribas, J.; Escuer, A.; Monfort, M.; Vicente, R.; Cortes, R.; Lezama, L.; Rojo, T. *Coord. Chem. Rev.* **1999**, *195*, 1027.
(6) Decurtins, S.; Schmalle, H. W.; P., S.; Ensling, J.; Gütlich, P. *J. Am. Chem. Soc.* **1994**, *116*, 9521.
(7) Armentano, D.; De Munno, G.; Lloret, F.; Palii, A. V.; Julve, M. *Inorg. Chem.* **2002**, *41*, 2007.
(8) For exceptions to weak exchange coupling through polyatomic, diamagnetic ligands, see the following and references therein: Ung, V. A.; Thompson, A.; Bardwell, D. A.; Gatteschi, D.; Jeffery, J. C.; McCleverty, J. A.; Totti, F.; Ward, M. D. *Inorganic Chemistry* **1997**, *36*, 3447.
(9) Manriquez, J. M.; Yee, G. T.; McLean, R. S.; Epstein, A. J.; Miller, J. S. *Science* **1991**, *252*, 1415.
(10) Caneschi, A.; Gatteschi, D.; Sessoli, R.; Rey, P. *Acc. Chem. Res.* **1989**, *22*, 392.
(11) Iwamura, H.; Inoue, K.; Haymizu, T. *Pure Appl. Chem.* **1996**, *68*, 243.
(12) Shultz, D. A. *Comments Inorg. Chem.* **2002**, *23*, 1.
(13) Hicks, R. G. *Aust. J. Chem.* **2001**, *54*, 597.

metal−radical coupling approach has resulted in magnetically ordered systems, with a high ordering temperature of 46 K.[14] Electroactivity is another attractive feature common to many classes of paramagnetic ligands, and is a key element in the mechanism of valence tautomerism.[15,16]

An alternative to the "solid-state approach" to magnetic materials is the synthesis of single molecules having both a high-spin ground-state and appreciable magneto-anisotropy. Such molecules have been termed "single-molecule magnets."[17] If appropriately designed molecules can be prepared, then individual molecules could be magnetized, thus obviating the need for extended solids and long-range magnetic ordering.

The successful creation of novel materials and magnetizable solids using either the extended-solid or the single-molecule approach necessitates the search for new paramagnetic ligands. Along these lines, we recently reported the preparation and magnetic properties, of nitronyl nitroxide-semiquinone (NN-SQ) complexes of Zn^{II} and Cu^{II}.[18] Analysis of the variable-temperature magnetic susceptibility data suggested strong intraligand NN-SQ exchange coupling. Variable-temperature variable-field magnetic circular dichroism studies of the Cu^{II} derivative were reported subsequently and illustrated the robustness of the exchange couplings in frozen solution and polymer matrices, where NN-SQ bond torsions are likely to deviate from values observed in the solid state.[19] To continue our study of (NN-SQ)M complexes, we report molecular structures for five-coordinate first-row M^{II} (M^{II} = Mn, Co, Ni, and Cu) complexes of NN-SQ. A six-coordinate Ni^{II} species has also been prepared, but X-ray quality crystals could not be obtained. Our Mn complex is the first structurally and magnetically characterized mono-SQ-Mn^{II} species. We also report the preparation, molecular structure and intra-ligand exchange coupling constant in a phenyl-spaced derivative of NN-SQ: **(NN-PhSQ)ZnTp^{Cum,Me}**. Our experimental results are accompanied by spin dimer analysis based on extended Hückel computations. Our results constitute the first magnetostructural correlations in a series of biradical-metal ion complexes. This combined experimental/theoretical approach has shown to be successful in simpler systems, most notably halide-bridged dinuclear copper(II) complexes.[20,21] Our results confirm the strong ferromagnetic NN-SQ exchange coupling that is insensitive to NN-SQ bond torsions. Finally, we illustrate that intraligand exchange coupling is of paramount importance in stabilizing high-spin states of mixed metal−biradical complexes.

Experimental Section

General. Unless noted otherwise, reactions were carried out in oven-dried glassware under nitrogen atmosphere. THF and toluene were distilled under argon from sodium benzophenone ketyl, and acetonitrile,

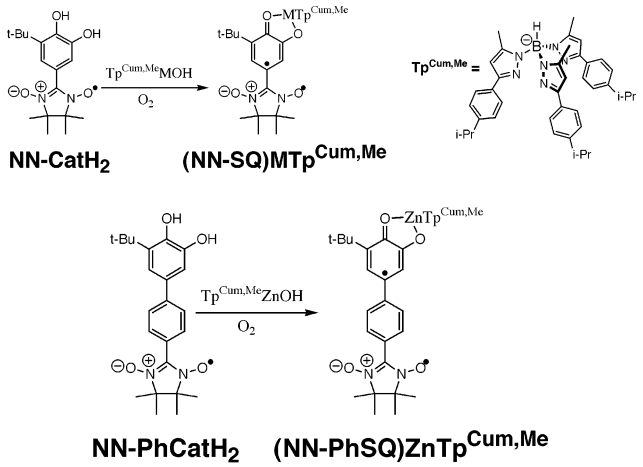

methylene chloride, and methanol were distilled from CaH_2 under argon. *tert*-Butyllithium (1.5 M in pentane) was used as received from Acros Chemical. Other chemicals were purchased from Aldrich Chemical Co. Column and radial chromatography were carried out using silica gel (230−400 mesh for column). X-Band EPR spectroscopy and electrochemistry were performed as described previously.[22] Fluid solution EPR spectra were simulated using WinSim.[23] NMR spectra were recorded at 300 MHz for ^{1}H NMR and 75 MHz for ^{13}C NMR in $CDCl_3$ solution if not otherwise specified. Elemental analyses were performed by Atlantic Microlab, Inc., Norcross, GA. Mass spectrometry was carried out at the NC State University Mass Spectrometry Facility. UV−visible spectra were collected on either an OLIS-converted Cary 14, or on a Hitachi U-3501 double beam UV−vis−NIR spectrophotometer equipped to collect data in the wavelength range from 180 to 3200 nm.

Synthesis. Catechol **NN-CatH$_2$** and the corresponding metal complexes were prepared as described previously,[18] and the synthesis write-ups for new compounds can be found in the Supporting Information.

Crystallographic Structure Determinations. Experimental information for the structure determinations of the metal complexes can be found in Supporting Information.

Magnetic Susceptibility Measurements. Magnetic susceptibilities were measured on a Quantum Design MPMS-XL7 SQUID magnetometer using an applied field of 0.5 T for Curie plots. Saturation magnetization values (see Supporting Information) are consistent with the spin of the ground states as described below. Microcrystalline samples were loaded into the sample space of a Delrin sample holder and mounted to the sample rod using string. Data were corrected for sample holder and molecular diamagnetism using Pascal's constants. The decrease in the χT data at low temperatures was accounted for with a Weiss correction, using the expression $\chi_{eff} = \chi/(1 - \vartheta\chi)$, where $\vartheta = 2zJ'_{inter}/(Ng^2\beta^2)$.[24] The origin of J'_{inter} may be zero-field splitting, intermolecular interaction, saturation effects or some combination of all three.[25] The other terms have their usual meaning.[24] The data are plotted as χT vs T (Figure 2), except for **(NN-SQ)NiTp^{Cum,Me}** which is also displayed as χ vs T in Figure 4.[26]

(14) Inoue, K.; Hayamizu, T.; Iwamura, H.; Hashizume, D.; Ohashi, Y. *J. Am. Chem. Soc.* **1996**, *118*, 1803.
(15) Shultz, D. A. Valence Tautomerism in Dioxolene Complexes of Cobalt. In *Magnetism: Molecules to Materials II: Molecule-Based Materials*; Miller, J. S., Drillon, M., Eds.; Wiley-VCH: New York, 2001; pp 281−306.
(16) Pierpont, C. G. *Coord. Chem. Rev.* **2001**, *216*, 99.
(17) Christou, G.; Gatteschi, D.; Hendrickson, D. N.; Sessoli, R. *MRS Bulletin* **2000**, 66.
(18) Shultz, D. A.; Bodnar, S. H.; Vostrikova, K. E.; Kampf, J. W. *Inorg. Chem.* **2000**, *39*, 6091.
(19) Depperman, E.; Bodnar, S. H.; Vostrikova, K. E.; Shultz, D. A.; Kirk, M. L. *J. Am. Chem. Soc.* **2001**, *123*, 3133.
(20) Crawford, V. H.; Richardson, H. W.; Wasson, J. R.; Hodgson, D. J.; Hatfield, W. E. *Inorg. Chem.* **1976**, *15*, 2107.
(21) Hay, P. J.; Thibeault, J. C.; Hoffmann, R. *J. Am. Chem. Soc.* **1975**, *97*, 4884.
(22) Shultz, D. A.; Farmer, G. T. *J. Org. Chem.* **1998**, *63*, 6254.
(23) Duling, D. *EPR Calculations for MS-Windows NT/95 Software Tools*, Version 0.96 ed.; Public EPR Software Tools, National Institute of Environmental Health Sciences, National Institutes of Health: Triangle Park, NC, 1996.
(24) O'Connor, C. J. *Prog. Inorg. Chem.* **1982**, *29*, 203.
(25) Caneschi, A.; Dei, A.; Mussari, C. P.; Shultz, D. A.; Sorace, L.; Vostrikova, K. E. *Inorg. Chem.* **2002**, *41*, 1086. Note that these authors used $H = \pm JS_1 \cdot S_2$. For comparison of J-values, we have recast their experimentally determined exchange parameters using a $H = -2JS_1 \cdot S_2$ exchange Hamiltonian.
(26) For antiferromagnetically coupled homospin complexes, the χ vs T plot is often displayed since a maximum is observed in χ, and is therefore preferable for fitting the data. However, the strongly paramagnetic ground state dominates the shape of the χ vs T plot for all complexes except **(NN-SQ) NiTp^{Cum,Me}** (see text), where no maximum in χ vs T is observed. Thus, the curvature of the χT vs T plots are greater and provide for better analysis of the data.

Scheme 1

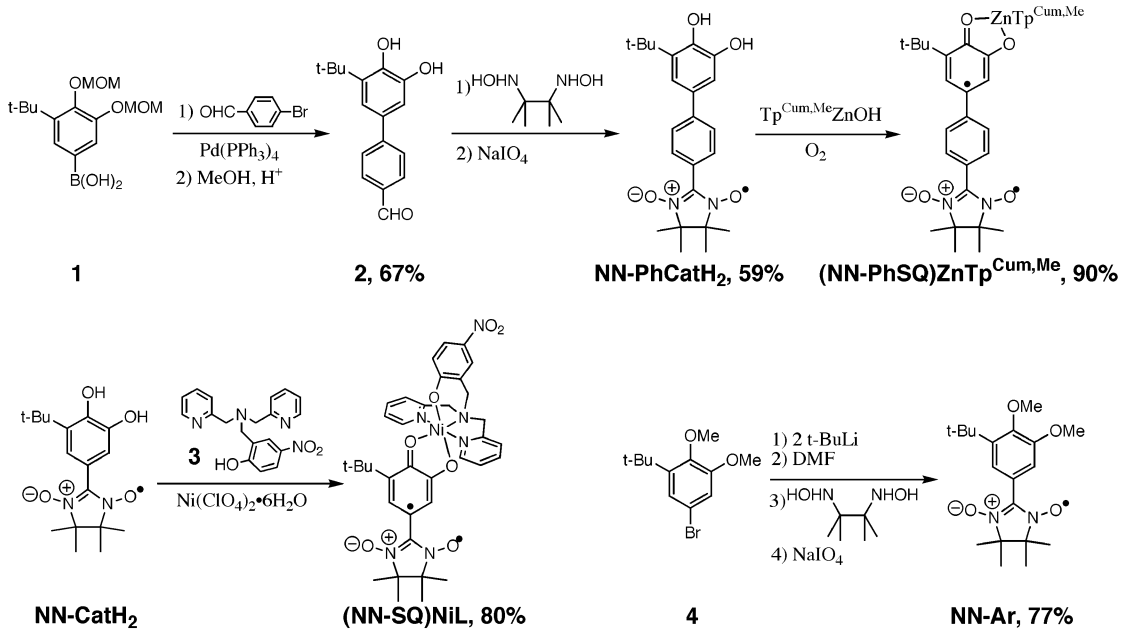

Extended Hückel Calculations. For a number of different magnetic solids, it has been shown that trends in spin exchange interactions are well described by spin dimer analysis based on extended Hückel (EH) calculations.[27] Thus, we performed EH calculations on **(NN-SQ)-MTp^{Cum,Me}** to determine the trend in both sign and magnitude of exchange coupling between metal ion and NN-SQ. The crystal structures of these compounds were used as structural inputs, and fragment molecular orbital analysis calculations (see below) were carried out by employing the *CAESAR* program package.[28] The results are displayed in Table 3.

Results and Analysis

Synthesis. Catechol **NN-CatH$_2$** and the corresponding metal complexes were prepared as described previously.[18] Despite several attempts, we have been unable to prepare the Fe^{II} complex of NN-SQ.[29] Because iron(II) offers the possibility for either an intermediate spin complex, a spin-crossover complex, or a complex having large zero-field splitting, synthetic efforts to prepare an Fe^{II} complex of NN-SQ continue. The phenyl-spaced derivative of **NN-CatH$_2$**, **NN-PhCatH$_2$**, its **ZnTp^{Cum,Me}** complex, and **(NN-SQ)NiL** having a six-coordinate Ni^{II} were prepared according to the Scheme 1.

Boronic ester **1**[30] was reacted with commercially available 4-bromobenzaldehyde under Suzuki coupling conditions,[31] followed by deprotection to give aldehyde **2** in excellent yield. Compound **2** was reacted with 2,3-dimethyl-2,3-bis(hydroxyamino)butane,[32] followed by oxidation to yield **NN-PhCatH$_2$**. Complex formation with HOZnTp^{Cum,Me} [33] followed standard procedures.[34,35]

The complex **(NN-SQ)NiL** was prepared from ligand **3**,[36] nickel(II)perchlorate, and **NN-CatH$_2$** in the presence of potassium hydroxide.

A model compound, **NN-Ar** (Ar = 5-*tert*-butyl-3,4-dimethoxyphenyl) was prepared as shown in Scheme 1. Bromide **4**[31] was subjected to lithium−halogen exchange, and the resulting aryl−lithium reagent was quenched with DMF to give the corresponding aldehyde. The aldehyde was subsequently transformed into **NN-Ar** using standard protocol.

X-ray Crystallography. The crystal structure of **(NN-SQ)-ZnTp^{Cum,Me}** was reported previously, and thermal ellipsoid plots of the new compounds are shown in Figure 1. Crystallographic data are collected in Table 1. A tabular collection of bond lengths and torsion angles can be found in the Supporting Information.

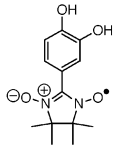

Magnetic Susceptibility. The magnetic susceptibility data for all of the compounds are plotted in Figures 2 and 4. The intraligand exchange coupling has previously been shown to be strongly ferromagnetic in **(NN-SQ)ZnTp^{Cum,Me}**,[18] with only the triplet being populated at temperatures as high as 300 K. Therefore, a lower limit of $J_{NN\text{-}SQ}$ was estimated to be +310 cm^{-1}. Because of the strong intraligand exchange coupling, the exchange Hamiltonian in eq 1 has been used for all of the **(NN-SQ)ML** complexes and the data have been fit using the field-independent van Vleck expression. Here, J is the exchange interaction between the paramagnetic metal and the strongly

(27) Koo, H.-J.; Whangbo, M.-H. *Inorg. Chem.* **2001**, *40*, 2161.
(28) Ren, J.; Liang, W.; Whangbo, M.-H. *Crystal and Electronic Structure Analysis Using CAESAR*; PrimeC, 1998.
(29) The crude reaction mixture shows none of the characteristic NN-SQ electronic absorption bands, rather a broad band centered near 16700 cm^{-1} (600 nm), consistent with the **(NN-Cat)Fe^{III}Tp^{Cum,Me}** form, see: Heistand, R. H., II; Lauffer, R. B.; Fikrig, E.; Que, L., Jr. *J. Am. Chem. Soc.* **1982**, *104*, 2789.
(30) Shultz, D. A.; Hollomon, M. G. *Chem. Mater.* **2000**, *12*, 580.
(31) Shultz, D. A.; Boal, A. K.; Driscoll, D. J.; Kitchin, J. R.; Tew, G. N. *J. Org. Chem.* **1995**, *60*, 3578.
(32) Vostrikova, K. E.; Hirel, C.; Pecaut, J.; Rey, P. *Chem. Eur. J.* **2001**, *7*, 2007.
(33) Ruf, M.; Weis, K.; Vahrenkamp, H. *J. Chem. Soc., Chem. Commun.* **1994**, 135.
(34) Shultz, D. A.; Bodnar, S. H.; Kumar, R. K.; Kampf, J. W. *J. Am. Chem. Soc.* **1999**, *121*, 10664.
(35) Ruf, M.; Noll, B. C.; Groner, M. D.; Yee, G. T.; Pierpont, C. G. *Inorg. Chem.* **1997**, *36*, 4860.
(36) Uma, R.; Viswanathan, R.; Palaniandavar, M.; Lakshminarayanan, M. *J. Chem. Soc., Dalton Trans.* **1994**, 1219.

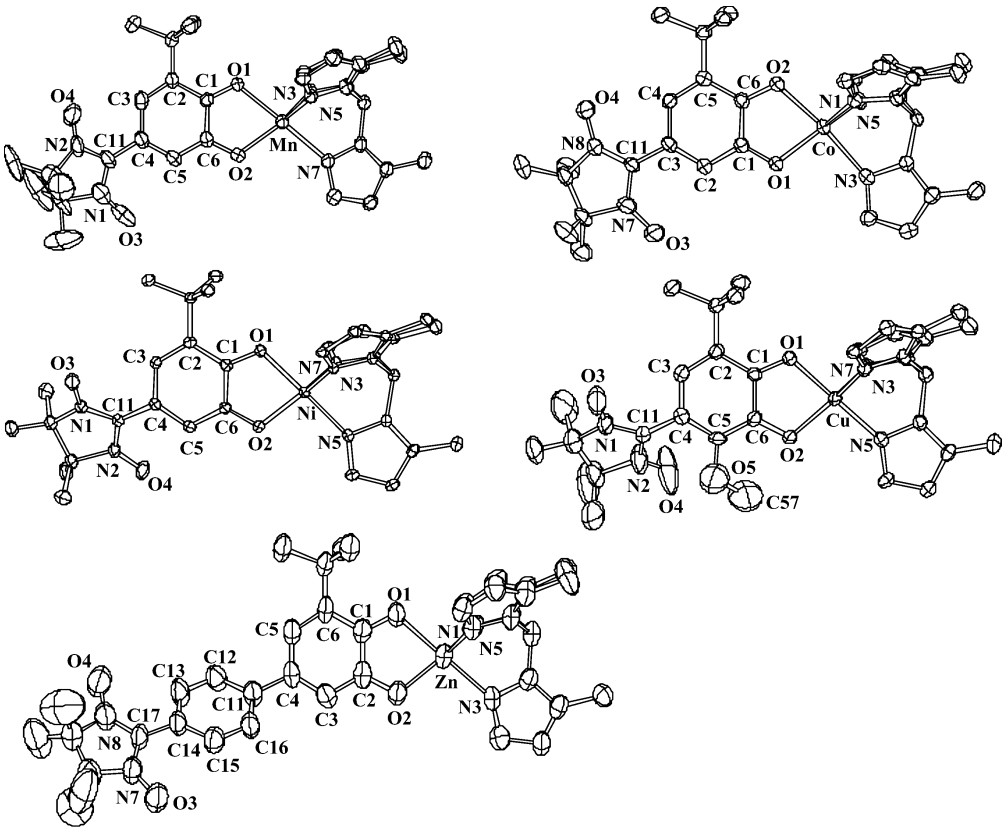

Figure 1. Thermal ellipsoid drawings of **(NN-SQ)MTp^{Cum,Me}** and **(NN-PhSQ)ZnTp^{Cum,Me}**. Cumenyl groups and hydrogens have been omitted for clarity.

Table 1. Crystallographic Data for **(NN-SQ)MnTp^{Cum,Me}**, **(NN-SQ)CoTp^{Cum,Me}**, **(NN-SQ)NiTp^{Cum,Me}**, and **[NN-SQ(OMe)]CuTp^{Cum,Me}** and **(NN-PhSQ)ZnTp^{Cum,Me}**

chemical formula	$C_{56}H_{69}BMnN_8O_4$ **(NN-SQ)MnTp^{Cum,Me}**	$C_{56}H_{69}BCoN_8O_4$ **(NN-SQ)CoTp^{Cum,Me}**	$C_{56}H_{69}BN_8NiO_4$ **(NN-SQ)NiTp^{Cum,Me}**	$C_{57}H_{71}BCuN_8O_5$ **[NN-SQ(OMe)]CuTp^{Cum,Me}**	$C_{62}H_{73}BN_8O_4Zn$ **(NN-PhSQ)ZnTp^{Cum,Me}**
a/Å	12.828(5)	12.582(3)	12.1536(9)	12.2081(8)	14.230(5)
b/Å	17.777(7)	17.693(4)	13.2557(10)	13.2504(9)	17.950(6)
c/Å	24.075(9)	24.370(5)	17.3931(12)	17.3758(11)	25.171(8)
α/deg	90	90	96.801(10)	96.958(3)	80.091(5)
β/deg	104.274(6)	98.401(4)	107.518(10)	105.603(3)	75.019(6)
γ/deg	90	90	98.335(10)	99.577(2)	82.382(6)
V/Å^3	5321(4)	5366.9(19)	2604.6(3)	2628.4(3)	6092(4)
Z	4	4	2	2	4
formula weight	983.94	987.93	987.71	1022.57	1070.46
space group	monoclinic $P2_1/c$	monoclinic $P2_1/c$	triclinic $P\bar{1}$	triclinic $P\bar{1}$	triclinic $P\bar{1}$
T/K	158(2)	158(2)	108(2)	158(2)	158(2)
ρ_{calcd}/g cm^{-3}	1.228	1.223	1.259	1.292	1.167
R^a	0.1258[d]	0.1086[d]	0.0459[d]	0.0993[d]	0.1545[d]
$R_w{}^b$	–	–	–	–	–
wR2 (F^2)[c]	0.2668	0.2306	0.0818	0.2100	0.2512

[a] $R = \Sigma(|F_o| - |F_c|)/\Sigma F_o$. [b] $R_w = [\Sigma\, w(F_o - F_c)/(\Sigma w F_o^2)]^{1/2}$. [c] wR2 $= [\Sigma w(F_o - F_c)/(\Sigma w F_o^4)]^{1/2}$; GoF $= S = [\Sigma w(F_o - F_c)/(n - p)]^{1/2}$, where n = number of reflections and p = number of parameters. [d] For $[F^2 > 2\sigma(F^2)]$.

coupled NN-SQ ligand, $\hat{S}_1$ is the spin operator for the NN-SQ ligand ($S_{NN\text{-}SQ} = 1$), and $\hat{S}_2$ is the spin operator for the metal ion. A similar approach has been used for other high-spin organic molecules.[37] The best-fit parameters for the χT data are given in Table 2, and qualitative energy level diagrams are given in Figure 3.

$$H = -2J\hat{S}_1\cdot\hat{S}_2 \qquad (1)$$

The χT product for **(NN-SQ)MnTp^{Cum,Me}** is given by eq 2:

$$\chi T = \frac{Ng^2\beta^2}{3k}\,\frac{15 + 52.5\,e^{-5J/kT} + 126\,e^{-12J/kT}}{4 + 6\,e^{-5J/kT} + 8\,e^{-12J/kT}} \qquad (2)$$

where $\boldsymbol{J}$ is the metal−ligand exchange coupling constant and the other symbols have their usual meaning. Inspection of Figure 2 indicates that the exchange interaction is clearly antiferromagnetic, yielding an $S_T = {}^3/_2$ ground state which lies $5\boldsymbol{J}$ below the sextet ($S_T = {}^5/_2$) and $12\boldsymbol{J}$ below the $S_T = {}^7/_2$ state. The exchange coupling constant was determined from the best fit of eq 2 to the data, yielding $\boldsymbol{J} = -41.3$ cm^{-1}.

The χT vs T data for the five-coordinate nickel complex, **(NN-SQ)NiTp^{Cum,Me}** (Figure 2) reveal the presence of dominant antiferromagnetic interactions between $S_{Ni} = 1$ and $S_{NN\text{-}SQ} = 1$ spin centers leading to a diamagnetic $S_T = 0$ ground state. Additionally, a small paramagnetic impurity manifests itself in

(37) Jacobs, S. J.; Shultz, D. A.; Jain, R.; Novak, J.; Dougherty, D. A. *J. Am. Chem. Soc.* **1993**, *115*, 1744.

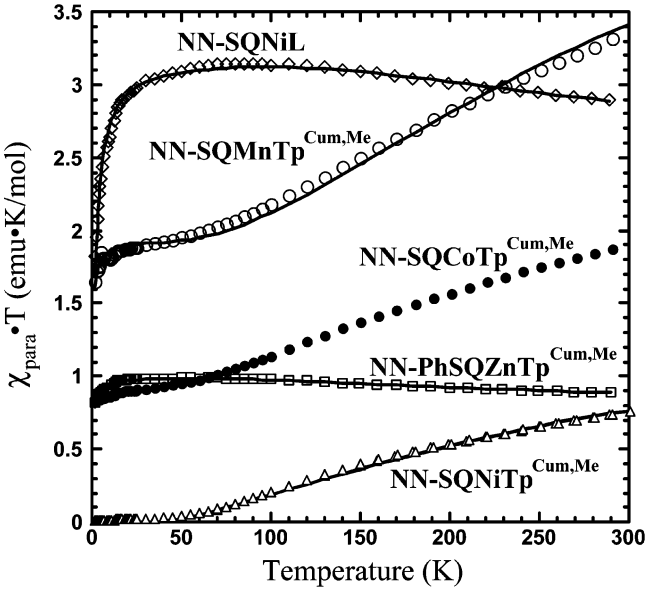

Figure 2. $\chi_{para}T$ vs T plots for **(NN-SQ)MTp^{Cum,Me}**, **(NN-PhSQ)-ZnTp^{Cum,Me}**, and **(NN-SQ)NiL**.

the form of a Curie tail in the χ vs T data at low temperatures (see Figure 4).

Therefore, the susceptibility data for **(NN-SQ)NiTp^{Cum,Me}** were initially fit with a model that takes into account a paramagnetic impurity term. However, best fits to the data yielded unusually low g-values ($g \approx 1.7$) for a five-coordinate Ni^{II}-biradical pair ($g_{Ni} > 2.0$, $g_{NN\text{-}SQ} \approx 2.0$),[38] requiring reassessment of the model employed. Since the $S_{Ni} = 1$ and $S_{NN\text{-}SQ} = 1$, spin centers in **(NN-SQ)NiTp^{Cum,Me}** are related by neither an inversion center nor a C_n rotation axis, antisymmetric exchange interactions[39] may be operative. This additional term in the spin Hamiltonian is given by:[39]

$$H_{antisymm} = d_{ab}[S_a \times S_b] \tag{3}$$

Antisymmetric exchange describes a mechanism for the mixing of two states that differ in spin multiplicity. In the case of **(NN-SQ)NiTp^{Cum,Me}**, the ground state is no longer strictly diamagnetic due to the triplet admixture, resulting in a finite value for the low-temperature susceptibility. Thus, the susceptibility expression was modified to include a Boltzmann-weighted paramagnetic contribution to the low-temperature susceptibility in addition to the paramagnetic impurity term.

$$\chi = \frac{Ng^2\beta^2}{3kT}\left[\frac{6\,e^{-2J/kT} + 30\,e^{-6J/kT}}{1 + 3\,e^{-2J/kT} + 5\,e^{-6J/kT}}\right] + \frac{Ng^2\beta^2 S(S+1)}{3kT} + \frac{C_{antisymm}}{1 + 3\,e^{-2J/kT} + 5\,e^{-6J/kT}} \tag{4}$$

The best-fit of eq 4 to the susceptibility data yielded $g = 1.8$, $J = -91$ cm^{-1}, and $C_{antisymm} = 540 \times 10^{-6}$ cm^3/mol, with <1% of an $S = 1$ impurity that presumably results from the uncoupled spin components. The best-fit parameters presented in Table 2 are an average of the values obtained from χ vs T and χT vs T fits.

The data for six-coordinate nickel complex **(NN-SQ)NiL** were fit using eq 5:

$$\chi T = \frac{Ng^2\beta^2}{3k}\frac{6\,e^{-2J/kT} + 30\,e^{-6J/kT}}{1 + 3\,e^{-2J/kT} + 5\,e^{-6J/kT}} \tag{5}$$

The χT product is consistent with ferromagnetic coupling between nickel and NN-SQ spins. The best-fit of eq 5 to the susceptibility data yielded $g = 2.04$ and $J = +79.9$ cm^{-1}.

Finally, for **(NN-PhSQ)ZnTp^{Cum,Me}**, the ligand spins are ferromagnetically coupled and were fit with eq 6 by using $J = J_{NN\text{-}SQ}$ and by fixing $g = 2$. Thus, for the phenyl-spaced derivative of the NN-SQ ligand, the intraligand exchange interaction is attenuated, and the excited singlet lies $2J_{NN\text{-}SQ} = 200$ cm^{-1} above the ground-state triplet.

$$\chi T = \frac{Ng^2\beta^2}{3k}\frac{6}{3 + e^{-2J/kT}} \tag{6}$$

Interestingly, the χT data for **(NN-SQ)CoTp^{Cum,Me}** cannot be fit using simple spin-only susceptibility expressions, and this is likely a manifestation of large spin−orbit coupling effects within the Co^{II} ^4T parent ground state. However, the metal−ligand interaction is clearly antiferromagnetic, and this is consistent with Pierpont's **(3,5-DBSQ)CoTp^{Cum,Me}** complex.[35]

Trends in Antiferromagnetic Spin Exchange Interactions. The exchange interactions between the $S_{NN\text{-}SQ} = 1$ organic ligand NN-SQ and those of the divalent transition metal ion are antiferromagnetic for **(NN-SQ)NiTp^{Cum,Me}** ($J = -87.8$ cm^{-1}) and **(NN-SQ)MnTp^{Cum,Me}** ($J = -41.3$ cm^{-1}), but ferromagnetic for **[NN-SQ(OMe)]CuTp^{Cum,Me}** ($J = +75.6$ cm^{-1}). The exchange parameter J can be written as the sum of ferro- and antiferromagnetic comtributions ($J = J_F + J_{AF}$).[21,40] Often, the ferromagnetic term J_F is small, and J only becomes ferromagnetic when the antiferromagnetic term J_{AF} is negligible. Therefore, trends in metal−ligand antiferromagnetic exchange interactions can be discussed solely on the basis of the antiferromagnetic terms J_{AF}. The J-values of **(NN-SQ)MTp^{Cum,Me}** determined in the present work imply that the magnitude of antiferromagnetic exchange interaction between the spins of NN-SQ and M^{II} decreases in the order, **(NN-SQ)NiTp^{Cum,Me}** > **(NN-SQ)MnTp^{Cum,Me}** > **[NN-SQ(OMe)]CuTp^{Cum,Me}** and that the antiferromagnetic exchange interaction is very weak in **[NN-SQ(OMe)]CuTp^{Cum,Me}**. In this section we explore these implications by analyzing the experimentally determined metal−ligand exchange interactions present in the **(NN-SQ)MTp^{Cum,Me}** complexes.

Since we are interested in understanding qualitative trends in the magnetic properties of closely related systems, it is sufficient to estimate the relative magnitudes of the exchange interactions solely on the basis of extended Hückel calculations.[27] Consider that each spin carrier in an exchange-coupled dimer contains one unpaired electron and the two spin sites are represented by magnetic orbitals ϕ_a and ϕ_b (i.e., singly occupied molecular orbitals representing the spin sites a and b, respectively). If t_{ab} is the hopping integral (i.e., the resonance integral) between ϕ_a and ϕ_b, then the J_{AF} term is related to t_{ab} as:[21,41,42]

$$J_{AF} = -2t_{ab}^2/U_{eff} \tag{7}$$

(38) Benelli, C.; Dei, A.; Gatteschi, D.; Pardi, L. *Inorg. Chem.* **1990**, *29*, 3409. Note that these authors used $H = \pm JS_1 \cdot S_2$. For comparison of J-values, we have recast their experimentally determined exchange parameters using a $H = -2JS_1 \cdot S_2$ exchange Hamiltonian.
(39) Moriya, T. *Phys. Rev.* **1960**, *117*, 635.

Table 2. Fit Parameters from Variable-Temperature Magnetic Susceptibility Measurements

compound	g	J/cm^{-1}	zJ'_{inter}/cm^{-1}[a]	$C_{antisymm}$/emu·mol^{-1}[b]	ref
(NN-SQ)MnTp^{Cum,Me}	2.03 ± 0.005	−41.3 ± 0.5	−0.01 ± 0.004	−	this work
(NN-SQ)CoTp^{Cum,Me}	−	<0	−	−	this work
(NN-SQ)NiTp^{Cum,Me}	1.78 ± 0.03[b]	−87.8 ± 4.0[c]	+0.002 ± 0.001	5.0 ± 0.4 × 10^{-4}[b]	this work
[NN-SQ(OMe)]CuTp^{Cum,Me}	2.02 ± 0.001	+75.6 ± 1.0	−0.18 ± 0.02	−	ref 18
(NN-SQ)ZnTp^{Cum,Me}	−	> +300[c]	<0	−	ref 18
	−	+550[d]	−	−	this work
(NN-PhSQ)ZnTp^{Cum,Me}	2.0 (fixed)	+100.1 ± 3.2[a]	−0.26 ± 0.02	−	this work
(NN-SQ)NiL	2.06 ± 0.002	+78.6 ± 2.3	−0.31 ± 0.02	−	this work

[a] Intermolecular correction term, see Experimental Section. [b] Antisymmetric exchange contribution, see text. [c] Fit parameters are an average from the χT and χ vs T plots. [c] $J_{NN\text{-}SQ}$ intraligand coupling. [d] From eq 11, see text.

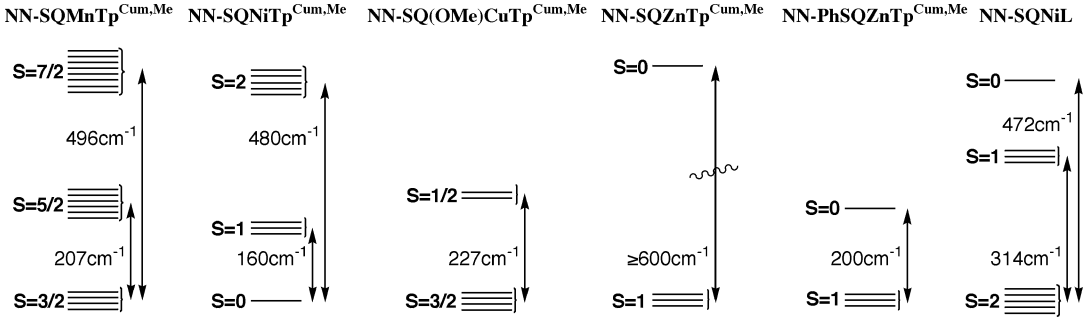

Figure 3. Energy gaps for spin states using $H = -2JS_1S_2$.

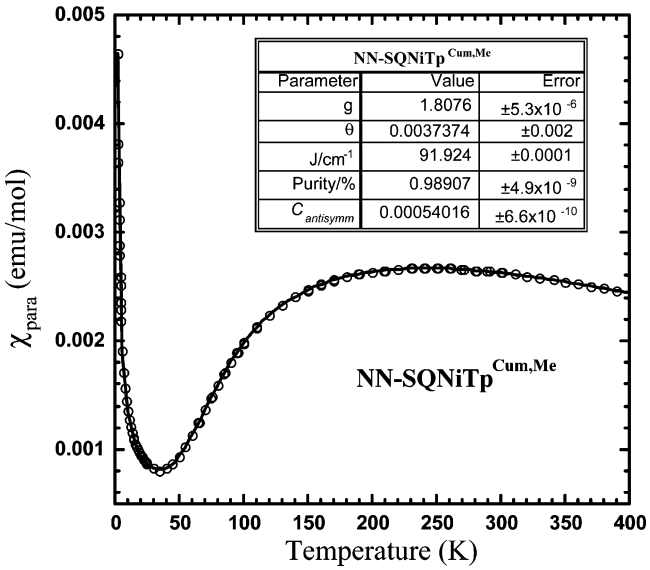

Figure 4. χ_{para} vs T plot for **(NN-SQ)NiTp^{Cum,Me}**.

where U_{eff} is the effective on-site repulsion, which should be nearly constant for closely related systems. (Note that eq 7 is valid only when the spin Hamiltonian is expressed as $\hat{H} = -2J\hat{S}_1\cdot\hat{S}_2$ instead of $\hat{H} = -J\hat{S}_1\cdot\hat{S}_2$.) In a magnetic dimer where superexchange interactions are operative, the two spin sites share at least one common atom so that their magnetic orbitals are not well defined for quantitative calculations of t_{ab}. In this case, the value of t_{ab} is determined indirectly by performing molecular orbital calculations for a spin dimer.[27,41] For example, when the two spin sites in an exhange-coupled dimer are equivalent, the t_{ab} integral is related to the spin−orbital interaction energy, Δe (i.e., the energy separation between the highest two singly occupied energy levels of a spin dimer) by $t_{ab} = \Delta e/2$. When two adjacent spin sites have m and n unpaired spins, respectively, the overall spin exchange parameter J is written as:[41,43]

$$J = \frac{1}{mn}\sum_{\mu=1}^{m}\sum_{\nu=1}^{n} J_{\mu\nu} \tag{8}$$

The estimation of qualitative trends in J on the basis of spin−orbital interaction energies has been discussed elsewhere.[44,45] However, this approach is more difficult to employ computationally for low-symmetry molecules such as **(NN-SQ)MTp^{Cum,Me}** (as Figure 6 would imply, vide infra). Thus we consider the average of the hopping integral squared, $\langle t^2\rangle$, defined by:

$$\langle t^2\rangle = \frac{1}{mn}\sum_{\mu=1}^{m}\sum_{\nu=1}^{n} t_{\mu\nu}^2 \tag{9}$$

Then the J_{AF} value is approximated by:

$$J_{AF} = -2\langle t^2\rangle/U_{eff} \tag{10}$$

Let us now consider how to estimate the $\langle t^2\rangle$ values for **(NN-SQ)MTp^{Cum,Me}**. The NN-SQ ligand contains two unpaired spins ($m = 2$), while the M^{II} ion has five unpaired spins for Mn^{II} ($n = 5$), two unpaired spins for Ni^{II} ($n = 2$), and one unpaired spin for Cu^{II} ($n = 1$). The primary orbital interactions between the (NN-SQ) ligand and the (M^{II}Tp^{Cum,Me})$^+$ fragment in **(NN-SQ)MTp^{Cum,Me}** involve the out-of-plane oxygen lone-pair orbitals of the SQ fragment of the NN-SQ ligand. The magnetic exchange interaction between the two spin sites of **(NN-SQ)-MTp^{Cum,Me}** involve the two magnetic orbitals $\phi_\mu = \phi_{NN}$ and ϕ_{SQ}, which are both π-type molecular orbitals. It is not

(40) Kahn, O.; Briat, B. *J. Chem. Soc., Faraday Trans. 2* **1976**, *72*, 268.
(41) Kahn, O. *Molecular Magnetism*; VCH: New York, 1993.
(42) Whangbo, M.-H.; Koo, H.-J. *Inorg. Chem.* **2002**, *41*, 3570.
(43) Charlot, M. F.; Kahn, O. *Nouv. J. Chim.* **1980**, *4*, 567.
(44) Koo, H.-J.; Whangbo, M.-H.; Coste, S.; Jobic, S. *J. Solid State Chem.* **2001**, *156*, 464.
(45) Dai, D.; Koo, H.-J.; Whangbo, M.-H. Solid State Chemistry of Inorganic Materials III. In *MRS Symposium Proceedings*; Geselbracht, M. J., Greedan, J. E., Johnson, D. C., Subramanian, M. A., Eds.; Materials Research Society: Warrendale, PA, 2001; Vol. 658, GG5.3.1−5.3.11.

Table 3. Comparison of the Calculated $\langle f^2 \rangle$ and J_{AF} Values of **(NN-SQ)MTp^{Cum,Me}** with Their Experimental ***J***-Values

M	m[a]	n[b]	$\langle f^2 \rangle$[c]/meV^2	J_{AF}[d]/cm^{-1}	J[e]/cm^{-1}
Mn	2	5	9700	−41.3	−41.3
Ni	2	2	16200	−68.9	−87.8
Cu	2	1	1300	−0.7	+75.6

[a] Number of ligand (NN-SQ) spins. [b] Number of metal ion spins. [c] Average of the hopping integral (resonance integral) squares. [d] Antiferromagnetic contribution to J from eq 10. [e] Experimental J-values.

straightforward to define the magnetic orbitals describing only the spins of the M^{II} ion site. If we require that the coordination sphere of the M^{II} ion be complete in the spin monomer of the M^{II} ion site, then the spin monomer must include orbitals on the NN-SQ ligand. However, the NN-SQ ligand also possesses unpaired spin ($S_{NN\text{-}SQ} = 1$). To avoid this conceptual difficulty, we will define the monomer fragment of the M^{II} site as (M^{II}Tp^{Cum,Me})$^+$ and the magnetic orbitals $\phi_\nu = \phi_M$ of this fragment as those orbitals that are the primary contributors to the singly filled d-block levels of **(NN-SQ)MTp^{Cum,Me}**. Therefore, there are five magnetic orbitals for the (Mn^{II}Tp^{Cum,Me})$^+$ fragment, two for (Ni^{II}Tp^{Cum,Me})$^+$, and one for (Cu^{II}Tp^{Cum,Me})$^+$. Within the extended Hückel formalism,[46] the $t_{\mu\nu}$ values between the orbitals ϕ_{SQ} and ϕ_M are easily evaluated by performing fragment molecular orbital analysis. Therefore the primary contribution to J_{AF} arises solely from interactions involving the ϕ_{SQ} orbital. The results are presented in Table 3.

Discussion

Molecular Structures. The bond lengths for the SQ rings of the NN-SQ complexes are consistent with the SQ oxidation state (i.e., M^{II}SQ and not M^{III}Cat, see Supporting Information).[47] However, there is a periodic variation in SQ-ring bond lengths that reflects interaction with the NN group. Previously, we defined this bond length deviation parameter ($\Sigma|\Delta_i|$) for new quinone-methide-semiquinone ($\Sigma|\Delta_i| = 0.279$ Å) and bis-(semiquinone) ($\Sigma|\Delta_i| = 0.116$ Å) ligands.[48] The $\Sigma|\Delta_i|$ value using average bond lengths for NN-SQ is 0.148 Å[49] and is consistent with an interaction between NN and SQ moieties that causes a moderate redistribution of electron density and therefore slightly alters bond lengths.

The torsion angles between the ONCNO chains and SQ ring planes are noteworthy. This torsion will modulate π-interaction between SQ and NN moieties and therefore controls intraligand exchange coupling.[50] These torsion angles vary from 0.5° to 36.1° (see Supporting Information). Since π-overlap varies as $\cos(\phi)$, and the intrinsic intraligand coupling is so strong, we feel that the effect of the observed torsions on intraligand exchange is negligible. The fact that we can successfully employ a one-J Heisenberg Hamiltonian for all complexes lends validity to our assertion.

The crystal structure of **[NN-SQ(OMe)]CuTp^{Cum,Me}** is unique in that it shows a methoxy group attached to the SQ ring. The reaction of methanol with the dioxolene ligand could have occurred during reaction, or during recrystalization. The primary effect this OMe group has on the molecule is to disrupt the conjugation between NN and SQ units by imposing a torsion angle of 36.1°. Despite this torsion, the intraligand exchange remains ferromagnetic, another testimony to the inherently strong NN-SQ interaction.

The metal coordination geometries of the **(NN-SQ)MTp^{Cum,Me}** complexes (M = Mn, Co, Ni) are axially elongated trigonal bipyramidal, with the NN-SQ ligand occupying positions on a vertical plane. On the other hand, **[NN-SQ(OMe)]CuTp^{Cum,Me}** is best described as a distorted square pyramid with the NN-SQ ligand occupying positions on the tetragonal plane.[35] The metal ligand bond lengths (r_{M-O} and $r_{M-N} \approx 2.1$ Å) are consistent with high-spin electronic configurations for M = Mn, Co, and Ni.[35,47,51−53] Because X-ray quality crystals of **(NN-SQ)NiL** could not be produced, we hypothesize that the metal geometry is nominally octahedral, and therefore that the Ni^{II} is high-spin.

Ligand Design Elements. Heterospin organic molecules are those with multiple, different spin-containing moieties.[18,22,54−58] To prepare robust, *high-spin* structures an active atom (one with positive spin density) of one radical group must be attached to an inactive atom (one with negative spin density) of another radical group.[59−62] This is the case for our NN-SQ ligand: nitronyl-nitroxides are known to have large negative spin density at the middle carbon of the ONCNO chain,[63] and SQ has positive spin density at the C5 position.[64]

From a molecular orbital perspective, the SQ SOMO can mix with both the NN SOMO-1 and the NN LUMO to yield nondisjoint biradical SOMOs ($\phi_{NN\text{-}SQ}$ and ϕ_{NN} in Figure 5). Such biradicals have nonzero exchange integrals and therefore possess triplet ground states.[59] The magnetic properties of **(NN-SQ)ZnTp^{Cum,Me}** are indeed consistent with a robust triplet ground-state configuration for NN-SQ.[18]

Features of the cyclic voltammograms and electronic absorption spectra (see Supporting Information) corroborate our suggested interaction between SQ and NN moieties, and a full spectroscopic study will be presented in detail in a separate manuscript.[65]

Intra-Ligand Exchange Couplings. Variable-temperature magnetic susceptibility measurements have allowed for the determination of only a lower limit for $J_{NN\text{-}SQ}$.[18] As a result, we wished to evaluate exchange coupling attenuation by addition of a phenyl ring between the SQ and NN groups. Since the

(46) Hoffmann, R. *J. Chem. Phys.* **1963**, *39*, 1397.
(47) Pierpont, C. G.; Lange, C. W. *Prog. Inorg. Chem.* **1994**, *41*, 331.
(48) Shultz, D. A.; Bodnar, S. H.; Kampf, J. W. *Chem. Commun.* **2001**, 93.
(49) For **(NN-PhSQ) ZnTp^{Cum,Me}**, $\Sigma|\Delta_i| = 0.164$ Å, but this may reflect the lower quality of structural data.
(50) Shultz, D. A. Conformational Exchange Modulation in Trimethylenemethane (TMM)-Type Biradicals. In *Magnetic Properties of Organic Materials*; Lahti, P., Ed.; Marcel Dekker: New York, 1999.
(51) Pierpont, C. G.; Buchanan, R. M. *Coord. Chem. Rev.* **1981**, *38*, 45.
(52) Attia, A. S.; Pierpont, C. G. *Inorg. Chem.* **1997**, *36*, 6184.
(53) Benelli, C.; Dei, A.; Gatteschi, D.; Pardi, L. *Inorg. Chem.* **1988**, *27*, 2831. Note that these authors used $H = \pm JS_1 \cdot S_2$. For comparison of J-values, we have recast their experimentally determined exchange parameters using a $H = -2JS_1 \cdot S_2$ exchange Hamiltonian.
(54) Kumai, R.; Matsushita, M. M.; Izuoka, A.; Sugawara, T. *J. Am. Chem. Soc.* **1994**, *116*, 4523.
(55) Inoue, K.; Iwamura, H. *Angew. Chem., Int. Ed. Engl.* **1995**, *34*, 927.
(56) Tanaka, M.; Matsuda, K.; Itoh, T.; Iwamura, H. *J. Am. Chem. Soc.* **1998**, *120*, 7168.
(57) Liao, Y.; Xie, C.; Lahti, P. M.; Weber, R. T.; Jiang, J.; Barr, D. P. *J. Org. Chem.* **1999**, *64*, 5176.
(58) Ionita, P.; Whitwood, A. C.; Gilbert, B. C. *J. Chem. Soc., Perkin Trans. 2* **2001**, *2*, 1453.
(59) Borden, W. T.; Davidson, E. R. *J. Am. Chem. Soc.* **1977**, *99*, 4587.
(60) Lahti, P. M.; Rossi, A. R.; Berson, J. A. *J. Am. Chem. Soc.* **1985**, *107*, 2273.
(61) Borden, W. T. *Diradicals*; Wiley: New York, 1982.
(62) Iwamura, H. *Pure Appl. Chem.* **1993**, *65*, 57.
(63) Pontillon, Y.; Akita, T.; Grand, A.; Kobayashi, K.; Lelievre-Berna, E.; Pecaut, J.; Ressouche, E.; Schweizer, J. *J. Am. Chem. Soc.* **1999**, *121*, 10126.
(64) Wheeler, D. E.; Rodriquez, J. H.; McCusker, J. K. *J. Phys. Chem. A* **1999**, *103*, 4101.
(65) Depperman, E. C.; Kirk, M. L.; Shultz, D. A. Manuscript in preparation.

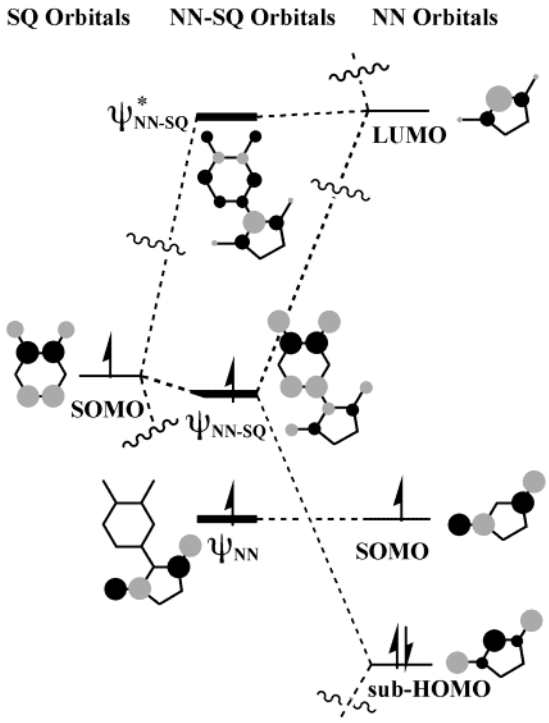

Figure 5. Qualitative MO diagram showing NN and SQ orbital mixing.

exchange interaction is anticipated to scale with the spin densities of the radical moieties,[37,61,66,67] we can estimate $J_{NN\text{-}SQ}$ with the relation:

$$J_{NN\text{-}PhSQ} = J_{NN\text{-}SQ}\left(\frac{\rho_{PhSQ}}{\rho_{SQ}}\right) = J_{NN\text{-}SQ}\left(\frac{a_{PhSQ}}{a_{SQ}}\right) \qquad (11)$$

where ρ_{PhSQ} is the spin density at the phenyl-C4′ position, and ρ_{SQ} is the C5 SQ spin density. Since these spin densities are directly proportional to the associated electron−nuclear hyperfine coupling constants,[68,69] the spin densities can be replaced with the corresponding coupling constants (a_i), which have been determined experimentally. Substituting the experimentally determined $J_{NN\text{-}PhSQ} = +100$ cm^{-1}, and the a_i values[70] into eq 11 gives $J_{NN\text{-}SQ} \approx +550$ cm^{-1}. Thus, the exchange parameter has been reduced by more than a factor of 5 compared to NN-SQ, consistent with diminished exchange caused by addition of the phenylene spacer. Modulation of the exchange interaction in biradicals by introducing spacers has been observed in Chichibabin hydrocarbon derivatives,[71] and in nitroxide triradicals.[11,72] The primary contribution to the reduction of the pairwise exchange interaction is a decrease in the SOMO−SOMO overlap density (caused by both additional atoms and bond torsions) and therefore attenuation of the exchange integral. Nevertheless, the +100 cm^{-1} ***J***-value for NN-PhSQ is still quite large.

Metal−Ligand Exchange Couplings. As mentioned above, the metal ion coordination geometries for the **(NN-SQ)-MTp^{Cum,Me}** complexes (M = Mn, Co, Ni) are distorted trigonal bipyramidal, except for the copper complex. For the trigonal bipyramidal complexes, assigning the long O−M−N axis as the molecular *z*-axis allows for a tentative description of the metal d-orbitals in pseudo-C_{3v} symmetry. Figure 6 depicts how the metal orbitals interact with the NN-SQ SOMO. The five pathway-dependent metal−ligand exchange interactions are anticipated to be either ferromagnetic for those metal orbitals that are orthogonal to the NN-SQ SOMO or antiferromagnetic for those metal orbitals that are symmetric with the NN-SQ SOMO.[41,73] Thus, the individual $J_{\mu\nu}$ expected to make ferromagnetic contributions to $J_{NN\text{-}SQ,M}$ are $J_{NN\text{-}SQ,d_z^2}$, $J_{NN\text{-}SQ,d_x^2-y^2}$, and $J_{NN\text{-}SQ,d_{xy}}$, while $J_{NN\text{-}SQ,d_{xz}}$, and $J_{NN\text{-}SQ,d_{yz}}$ are expected to make antiferromagnetic contributions to $J_{NN\text{-}SQ,M}$. For **[NN-SQ-(OMe)]CuTp^{Cum,Me}**, the metal coordination geometry is best described as a distorted square pyramid, and the magnetic orbital is expected to be $d_{x^2-y^2}$ which is orthogonal to the tetragonal plane and therefore orthogonal to the ligand magnetic orbitals. However, due to the low symmetry of the complexes, this approach may be oversimplified, and a more detailed description of the orbital nature of the metal−ligand exchange interaction has been provided using extended Hückel theory, vide supra.

Complex **(NN-SQ)MnTp^{Cum,Me}** is the first structurally characterized complex with one SQ-type ligand coordinated to *hs*-Mn^{II},[25] and the net antiferromagnetic exchange ($J = -41$ cm^{-1}) suggests that the antiferromagnetic $J_{\mu\nu}$ outweigh the ferromagnetic contributions to $J_{NN\text{-}SQ,M}$.

The susceptibility data for the complex **(NN-SQ)NiTp^{Cum,Me}** shows net antiferromagnetic metal−ligand exchange coupling and is consistent with interstate mixing described by an antisymmetric exchange term. Documented examples of antisymmetric exchange in binuclear centers are quite rare. However, anomalously low *g*-values recently observed in copper and iron−sulfur clusters have been attributed to the presence of antisymmetric exchange interactions.[74,75] The magnitude of the antisymmetric exchange parameter, $|d_{ab}|$, may be estimated by considering the following expression (Δg is the deviation of the average *g* of the two centers from the free electron $g_e = 2.0023$):[39,76]

$$|d_{ab}| \approx \frac{|\Delta g|}{g} J_{NN\text{-}SQ,Ni} \qquad (12)$$

Assuming $\Delta g \approx 0.1$, the antisymmetric exchange parameter could be as high as $|d_{ab}| \approx 4$ cm^{-1}. Since the antiferromagnetic exchange coupling between $S = 1$ Ni^{II} and $S = 1$ NN-SQ gives rise to a formally diamagnetic ground state, the small positive deviations from $\chi_{ave} = 0$ resulting from antisymmetric exchange are more readily observed than if the ground state were paramagnetic with a large increasing χ_{ave} as $T \rightarrow 0$. Therefore, the observed mixing of a singlet ground state with a low-lying

(66) Rajca, A. *Chem. Rev.* **1994**, *94*, 871.
(67) Rajca, A. High-Spin Polyradicals. In *Magnetic Properties of Organic Materials*; Lahti, P., Ed.; Marcel Dekker: New York, 1999; p 345.
(68) McConnell, H. M.; Chestnut, D. B. *J. Chem. Phys.* **1958**, *28*, 107.
(69) Wertz, J. E.; Bolton, J. R. *Electron Spin Resonance*; Chapman and Hall: New York, 1986.
(70) For the hyperfine coupling constant of SQ, we used the value for H4 reported in our previous work (3.33 G), and assumed negligible difference between the spin densities of C4 and C5: Shultz, D. A.; Boal, A. K.; Campbell, N. P. *Inorg. Chem.* **1998**, *37*, 1540−3; see also: Wheeler, D. E.; Rodriquez, J. H.; McCusker, J. K. *J. Phys. Chem. A* **1999**, *103*, 4101. For the H4′ hyperfine coupling constant for 3-*tert*-butyl-5-phenylsemiquione (0.6 G), we prepared the radical anion and simulated its fluid solution EPR spectrum, see Supporting Information.
(71) Waring, R. K.; Sloan, G. J. *J. Chem. Phys.* **1964**, *40*, 772.
(72) Kanno, F.; Inoue, K.; Koga, N.; Iwamura, H. *J. Phys. Chem.* **1993**, *97*, 13267.
(73) Kahn, O. *Angew. Chem., Int. Ed. Engl.* **1985**, *24*, 834.
(74) Clark, P. A.; Solomon, E. I. *J. Am. Chem. Soc.* **1992**, *114*, 1108.
(75) Sanakis, Y.; Macedo, A. L.; Moura, I.; Moura, J. J. G.; Papaefthymiou, V.; Münck, E. *J. Am. Chem. Soc.* **2000**, *122*, 11855.
(76) Gatteschi, D.; Sessoli, R.; Plass, W.; Miller, A.; Krickemeyer, E.; Meyer, J.; Solter, D.; Adler, P. *Inorg. Chem.* **1996**, *35*, 1926.

triplet excited state is more pronounced than the corresponding mixing would be had the ground-state been paramagnetic. Moreover, **(NN-SQ)NiTp^{Cum,Me}** has the lowest-lying excited state (Figure 3) of all the complexes and will therefore mix more strongly with the ground state. Antisymmetric exchange contributions undoubtedly occur in the manganese, cobalt, and copper complexes but are difficult to detect owing to their paramagnetic ground states and/or the fact that $\Delta g \ll 0.1$.

The χT data for six-coordinate **(NN-SQ)NiL** are consistent with orthogonal metal and ligand orbitals, and therefore also with six-coordinate Ni^{II} having d_{z^2} and $d_{x^2-y^2}$ magnetic orbitals.[53]

The ferromagnetic metal−ligand exchange coupling in **[NN-SQ(OMe)]CuTp^{Cum,Me}** was described previously[18,19] and is consistent with strong coupling between orthogonal NN-SQ and metal spins.

The Nature of the Metal−Ligand Exchange Interaction. The results of our extended Hückel calculations, summarized in Table 3, are in accord with both simple symmetry arguments and with experimental findings. The experimental ***J***-value of **(NN-SQ)MnTp^{Cum,Me}** is reproduced in terms of J_{AF} according to eq 10 (thereby ignoring the J_F terms), if U_{eff} is chosen as 3.76 eV. We employ this U_{eff} value to estimate the *relative* J_{AF} values of **(NN-SQ)NiTp^{Cum,Me}** and **[NN-SQ(OMe)]CuTp^{Cum,Me}**. The calculated J_{AF} values quantify the predicted antiferromagnetic exchange pathway contributions to $\boldsymbol{J}_{NN\text{-}SQ,M}$.[77] In fact, the antiferromagnetic exchange contributions to $\boldsymbol{J}_{NN\text{-}SQ,M}$ in the **(NN-SQ)MTp^{Cum,Me}** complexes are calculated to decrease in magnitude in the order, **(NN-SQ)NiTp^{Cum,Me}** > **(NN-SQ)MnTp^{Cum,Me}** > **[NN-SQ(OMe)]CuTp^{Cum,Me}**, and for the latter the antiferromagnetic exchange interaction is very weak. Qualitatively, J_{AF} is anticipated to be negligible in **[NN-SQ(OMe)]CuTp^{Cum,Me}** because the magnetic orbital, $\phi_{NN\text{-}SQ}$, of NN-SQ is nearly orthogonal to the d-block magnetic orbital of **[NN-SQ(OMe)]CuTp^{Cum,Me}**. The calculated J_{AF} of **(NN-SQ)MnTp^{Cum,Me}** is less than half that of **(NN-SQ)NiTp^{Cum,Me}**. According to eqs 9 and 10, this is understandable because there are more unpaired spins in the Mn^{II} ion site of **(NN-SQ)-MnTp^{Cum,Me}** than on the Ni^{II} ion site of **(NN-SQ)NiTp^{Cum,Me}**. Thus, despite the low molecular symmetries, the extended Hückel results support predictions based on higher-symmetry orbital overlap considerations as presented in Figure 6.

Comparison of Metal−Ligand Couplings with Those of Other SQ Complexes. The experimental metal−ligand exchange parameters reported in Table 2 may be compared to those of other M−SQ complexes[78] to obtain greater insight into the exchange interactions in (NN-SQ)M dyads. For example, Dei and Gatteschi reported five-coordinate Cu^{II} and Ni^{II} complexes of 3,5-di-*tert*-butylsemiquinone and found $\boldsymbol{J}_{SQ,Cu} = +52$ cm^{-1} for the copper complex and $\boldsymbol{J}_{SQ,M} < -300$ cm^{-1} for the nickel complex. [38] The same researchers also reported the magnetic properties of a *six*-coordinate Ni^{II} complex of 3,5-di-*tert*-butylsemiquinone for which the exchange is ferromagnetic with $\boldsymbol{J}_{SQ,Ni} > +200$ cm^{-1}.[53] Recently, one of us, in a collaborative effort, described the magnetic properties of six-coordinate Ni^{II} and five-coordinate Mn^{II} complexes of a tris(SQ) ligand.[25] The metal−ligand exchange parameters here were found to be: $\boldsymbol{J}_{SQ,Ni} = +87$ cm^{-1} and $\boldsymbol{J}_{SQ,Mn} = -175$ cm^{-1}.

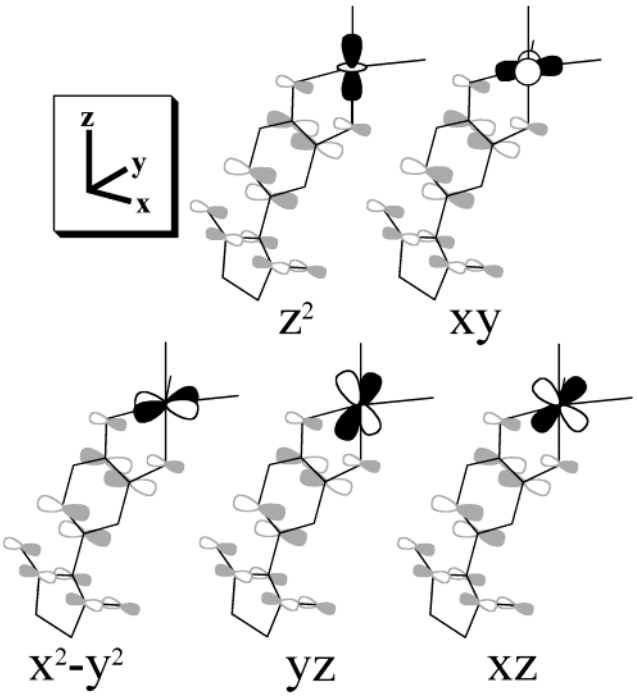

Figure 6. Qualitative trigonal bipyramidal MO diagram showing NN-SQ- and d-orbital mixing.

We can make direct comparisons between the M−SQ exchange interactions in M−SQ dyads and the (NN-SQ)M triads presented here by expressing the measured $\boldsymbol{J}_{NN\text{-}SQ,M}$ as $\boldsymbol{J}_{SQ,M}$ via diagonalization of the two-***J*** Heisenberg Hamiltonian at fixed $\boldsymbol{J}_{NN\text{-}SQ}$.[79] This is important, as structural and electronic parameters resulting from variations in the ancillary ligands and the extent of the direct exchange contribution, which scales according to the different M−L bond lengths,[80] may now be directly evaluated. If one uses limiting values of $\boldsymbol{J}_{NN\text{-}SQ} = +310$ cm^{-1} (the lower limit determined in our previous study)[18] and $\boldsymbol{J}_{NN\text{-}SQ} = +550$ cm^{-1} (estimated from eq 11), one can show that $\boldsymbol{J}_{SQ,Cu} = +187$ cm^{-1} and $+166$ cm^{-1} respectively for **[NN-SQ(OMe)]CuTp^{Cum,Me}**.[79] Thus, the ferromagnetic metal−SQ exchange interaction in the NN-SQ-Cu triad is more than *tripled* in magnitude compared to the previously mentioned five-coordinate copper complex[38] but is very close to the exchange interaction in (**3,5-DBSQ**)CuTp^{Cum,Me}.[35]

The spin state energies as a function of $\boldsymbol{J}_{SQ,Cu}$ at constant $\boldsymbol{J}_{NN\text{-}SQ}$ (= $+310$ cm^{-1} and $+550$ cm^{-1}) derived from this analysis are displayed graphically in Figure 7. Note that for $\boldsymbol{J}_{SQ,Cu} > +300$ cm^{-1}, the energy gap separating the ground quartet and the lowest doublet is independent of $\boldsymbol{J}_{SQ,Cu}$. This is an extremely important finding if one wishes to enhance the stability of high-spin states of multispin metal-radical complexes.

(77) These pathways are described by the Goodenough Kanamori rules, see the following. Ginsberg, A. P. *Inorg. Chim. Acta Rev.* **1971**, *5*, 45. Hatfield, W. E. In *Theory and Applications of Molecular Paramagnetism*; Boudreaux, E. A., Mulay, L. N., Eds.; Chapter 7, Properties of Condensed Compounds (Compounds with Spin Exchange); Wiley-Interscience: New York, 1976; pp 381−385.

(78) Pierpont, C. G.; Attia, A. S. *Collect. Czech. Chem. Commun.* **2001**, *66*, 33. Note that these authors used $H = \pm \boldsymbol{J} S_1 \cdot S_2$. For comparison of ***J***-values, we have recast their experimentally determined exchange parameters using a $H = -2\boldsymbol{J} S_1 \cdot S_2$ exchange Hamiltonian.

(79) For the copper complex, an 8 × 8 spin Hamiltonian exchange matrix, [$H = -2\boldsymbol{J}_{Cu,SQ} S_{Cu} \cdot S_{SQ} - 2\boldsymbol{J}_{NN\text{-}SQ} S_{SQ} \cdot S_{NN} - 2\boldsymbol{J}_{Cu,NN} S_{Cu} \cdot S_{NN}$] was derived using the uncoupled basis set $|S_{Cu}, M_{S,Cu}, S_{SQ}, M_{S,SQ}, S_{NN}, M_{S,NN}\rangle$. The matrix was diagonalized holding constant $\boldsymbol{J}_{Cu,NN} = 0$ and $\boldsymbol{J}_{NN\text{-}SQ} = +310$ ($+550$) cm^{-1}, and varying $\boldsymbol{J}_{Cu,SQ}$ until a value was obtained which gave eigenvalues matching the quartet-doublet splitting of 227 cm^{-1}. Analogous methods were used for the nickel complexes.

(80) Rodriguez, J. H.; Wheeler, D. E.; McCusker, J. K. *J. Am. Chem. Soc.* **1998**, *120*, 12051.

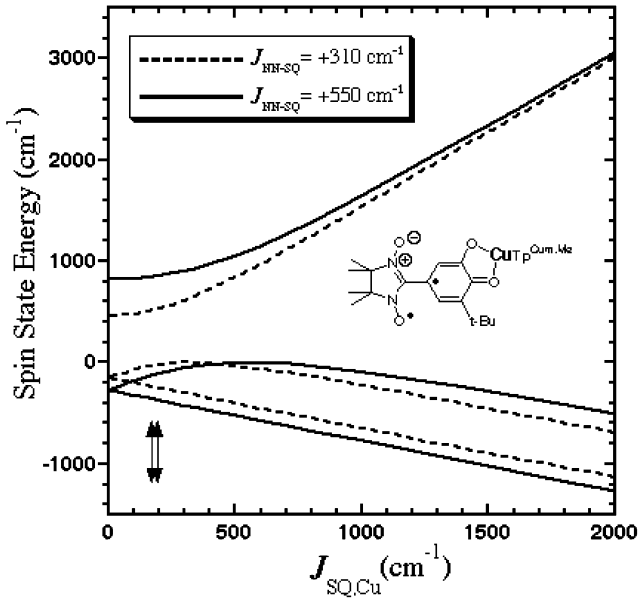

Figure 7. Spin state energies for **[NN-SQ(OMe)]CuTp^{Cum,Me}** as a function of $J_{SQ,Cu}$. J_{NN-SQ} = 310 cm^{-1} (- - -); J_{NN-SQ} = 550 cm^{-1} (—). The lowest-energy state is the quartet, with the two doublets lying higher in energy. The arrows in the lower left denote the limits of $J_{SQ,Cu}$.

Although strong metal−ligand coupling is obviously a necessary criterion, the intraligand coupling is of paramount importance for stabilizing the ground state *relative to the first excited spin-state.*

A similar analysis for **(NN-SQ)NiTp^{Cum,Me}** yields $J_{SQ,Ni}$ = −244 cm^{-1} and −525 cm^{-1} for J_{NN-SQ} = +310 cm^{-1} and J_{NN-SQ} = +550 cm^{-1}, respectively. For the six-coordinate coordinate complex, **(NN-SQ)NiL**, $J_{SQ,Ni}$ = +193 cm^{-1} and +320 cm^{-1} for J_{NN-SQ} = +550 cm^{-1} and J_{NN-SQ} = +310 cm^{-1}, respectively. These results are displayed graphically in Figure 8. Here it is clearly apparent that the electronic structure of the metal ion, which is a function of the coordination environment, can result in enormous changes in the sign and magnitude of the exchange interaction. This is a result of different $J_{\mu\nu}$ pathway contributions to the measured exchange, $J_{SQ,Ni}$, and is in direct accord with the Goodenough−Kanimoori rules[77] and extended Hückel analysis presented above. Nevertheless, $J_{SQ,Ni}$ values for our NN-SQ complexes are very close to reported values for complexes with similar coordination geometries, and we conclude that the NN group does not dramatically affect M−SQ exchange coupling.

Conclusions

We presented a comprehensive structural and magnetic study of isostructural first-row, high-spin transition metal complexes of the high-spin S = 1 NN-SQ ligand. The intraligand exchange interactions are strongly ferromagnetic in nature, and generally greater in magnitude than the metal−ligand exchange. The metal−ligand exchange interactions are in accord with magnetic orbital symmetry arguments within the active electron approximation. Despite the low symmetry (C_1) adopted by these complexes, extended Hückel calculations support high-symmetry arguments relating to the sign of the exchange parameter and have led to highly informative magnetostructural correlations in these hybrid metal−organic spin triads.

The low-temperature magnetic properties of the five-coordinate nickel complex, **(NN-SQ)NiTp^{Cum,Me}**, have been

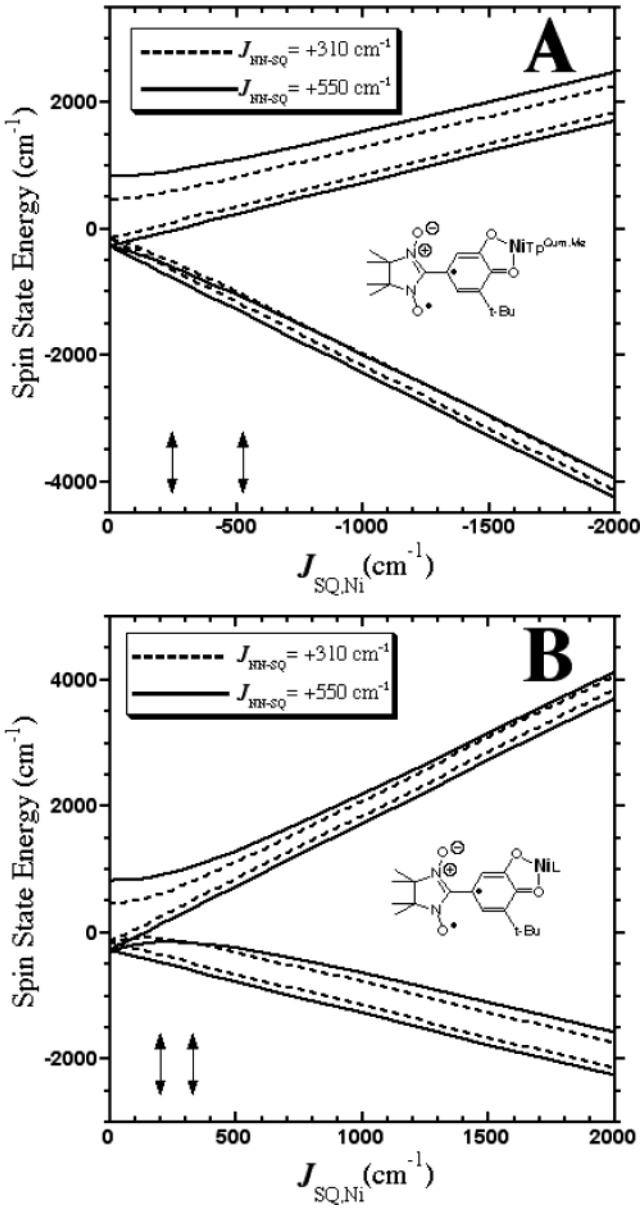

Figure 8. (A) Spin state energies for **(NN-SQ)NiTp^{Cum,Me}** as a function of $J_{SQ,Ni}$. J_{NN-SQ} = +310 cm^{-1} (- - -); J_{NN-SQ} = +550 cm^{-1} (—). The lowest-energy state is the singlet, with excited triplet, quintet, and triplet states, respectively. (B) Spin state energies for **(NN-SQ)NiL** as a function of $J_{SQ,Ni}$. J_{NN-SQ} = +310 cm^{-1} (- - -); J_{NN-SQ} = +550 cm^{-1} (—). The lowest-energy state is the quintet, with excited triplet, singlet, and triplet states, respectively. The arrows in the lower left denote the limits of $J_{SQ,Ni}$.

described with the addition of an antisymmetric exchange term. The presence of a singlet ground-state, coupled with a moderate exchange interaction conspire to allow interstate mixing with the low-lying triplet state. The general manifestations of this interstate mixing are a reduced g-value, and nonzero paramagnetic susceptibility in the formally singlet ground spin-state. However, this model is still insufficient to explanation the data for the corresponding cobalt complex. This is most likely an indication of substantial ground-state orbital moment for the d^7 cobalt complex. Antisymmetric exchange is less important for **(NN-SQ)MnTp^{Cum,Me}**, **[NN-SQ(OMe)]CuTp^{Cum,Me}**, and **(NN-SQ)NiL** due to the smaller Δg values and paramagnetic ground states.

The study also highlights the extreme importance of intraligand coupling for stabilization of the high-spin ground state of

multispin metal−radical complexes. This important finding has a profound impact on the design of high-spin metal−organic hybrid materials.

Acknowledgment. D.A.S. acknowledges the National Science Foundation (CHE-9910076; CHE-0091247 SQUID Magnetometer) for financial support and thanks the Camille and Henry Dreyfus Foundation for a Camille Dreyfus Teacher-Scholar Award. M.-H.W. acknowledges the financial support from the Office of Basic Energy Sciences, Division of Materials Sciences, U.S. Department of Energy, under Grant DE-FG02-86ER45259. M.L.K. acknowledges the National Institutes of Health GM-057378 for financial support.

Supporting Information Available: Synthetic details, crystallographic data, saturation magnetization plots, electronic spectra, cyclic voltammograms, and synthesis and EPR spectra for 3-*tert*-butyl-5-phenylsemiquinone (PDF/CIF). This material is available free of charge via the Internet at http://pubs.acs.org.

JA020715X